

Plasma Imaging by Using a High-speed Camera in the GAMMA 10 Tandem Mirror

Ryo YONENAGA, Yousuke NAKASHIMA, Nobuhiro NISHINO¹⁾, Yuta HIGASHIZONO²⁾,
Shinji KOBAYASHI³⁾, Katsuhiko HOSOI, Hiroki OZAWA, Takashi ISHII, Hisato TAKEDA,
Hiroyuki SHIDARA and Tsuyoshi IMAI

Plasma Research Center, University of Tsukuba, Tsukuba, Ibaraki 305-8577, Japan

¹⁾*Graduate school of Engineering, Hiroshima University, Hiroshima 739-8527, Japan*

²⁾*Advanced Fusion Research Center, Research Institute for Applied Mechanics, Kyushu University,
Kasuga, Fukuoka 816-8580, Japan*

³⁾*Institute of Advanced Energy, Kyoto University, Gokasho, Uji 611-0011, Japan*

(Received 7 December 2009 / Accepted 11 March 2010)

The two-dimensional (2-D) image of high temperature plasmas in the GAMMA 10 tandem mirror has been measured at the central-cell by using a high-speed camera. Temporal behavior of visible image in the central-cell was observed with high-speed camera in the experiment of antenna optimization of central-ECRH system. Observed results showed a significant dependence on the position of the central-ECRH antenna. We discuss the characteristics of the fluctuation in the light emission intensity and the correlation with the radial distribution of electron density in the period of ECRH.

© 2010 The Japan Society of Plasma Science and Nuclear Fusion Research

Keywords: GAMMA 10, tandem mirror, high-speed camera, visible-light emission, limiter-plasma interaction

DOI: 10.1585/pfr.5.S2045

1. Introduction

Two-dimensional (2-D) imaging of plasmas with a high-speed camera can capture the instantaneous 2-D plasma structure and provides useful information about shape, position and motion of the plasma. Recently, development of the performance in high-speed cameras enables us to effective means to analyze the 2-D imaging of the plasma behavior in detail. Therefore the 2-D imaging diagnostics with the high-speed camera has been employed in many fusion plasma devices [1–3].

The 2-D imaging of turbulent structure of high temperature plasmas in the GAMMA 10 Tandem Mirror has been measured at the central-cell by using a high-speed camera [4–6]. In GAMMA 10, plasmas are produced by ion cyclotron heating (ICH) and gas puffing and additional heating with electron cyclotron resonance heating (ECRH) and neutral beam injection (NBI) are supplied. The diagnostics of the plasma behavior with the high-speed camera give us lots of useful information for controlling the plasma condition about plasma response on the heating systems, gas puffing and limiters. In GAMMA 10, 2-D image of plasmas were observed by the high-speed camera in various experiments such as gas-puff-imaging (GPI) and hydrogen pellet injection [7].

The purpose of this study is to obtain some approach for understanding physical mechanism about plasma turbulent structure and its time-evolution by the observation

of plasma fluctuation and rotation. In this paper, we focus the plasma behavior in response to the injection of central-ECRH (C-ECRH) for bulk electron heating into the plasma under a good confinement condition obtained by plug-ECRH (P-ECRH) and barrier-ECRH (B-ECRH).

In the following Sec.2, experimental setup which consists of GAMMA 10 tandem mirror, the high-speed camera and the C-ECRH system is explained. Sec.3 describes the results of the experiment of antenna optimization in the C-ECRH system. In Sec.4, we discuss characteristics of fluctuation and the correlation between the light emission intensity and radial distribution of electron density. In Sec.5, the summary is shown.

2. Experimental Setup

2.1 GAMMA 10 tandem mirror

The GAMMA 10 tandem mirror is an open magnetic plasma-confining device with thermal barrier [8]. It consists of central-cell, anchor-cells, plug/barrier-cells and end-cells as shown in Fig. 1. As the midplane of the central-cell is defined as $z = 0$ cm, west and east directions correspond to plus and minus on z -axis, respectively. The central-cell is main region to confine plasma and 6 m in length and the diameter of 1 m. A central-limiter to limit the plasma diameter is located near the midplane ($z = +30$ cm) and 400 mm in diameter. In each anchor-cell, a minimum-B magnetic field is built for stabilizing the whole plasma. In the plug/barrier-cell, electrostatic po-

author's e-mail: yonenaga_ryo@prc.tsukuba.ac.jp

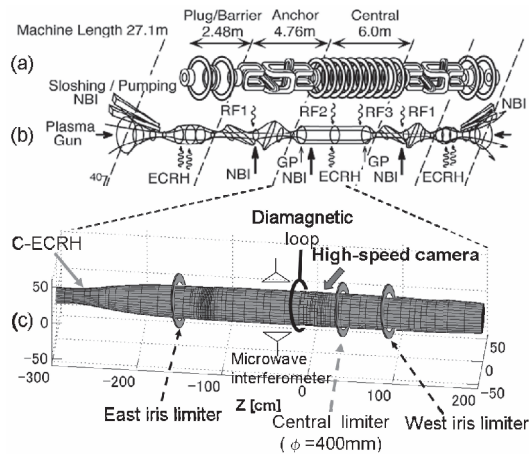


Fig. 1 Schematic view of GAMMA 10. (a) Coil arrangement, (b) magnetic flux tube and the location of plasma production and heating systems, (c) limiters and diagnostics in the central-cell.

tentials are built by P-/B-ECRH for confining the plasma in the central-cell. Primary plasma is built up by plasma guns located in both end-cells. The plasma is sustained by ICH and gas puffing. Additionally, C-ECRH and neutral beam injection (NBI) are supplied for the plasma heating in the central-cell.

2.2 High-speed camera and other diagnostics

The high-speed camera (MEMRECAM fx-K5, NAC Inc.) is mounted at the midplane of the central-cell ($z = 0$ cm). The framing speed of the high-speed camera is 40,000 frames per second and the imaging size is 144×192 pixels. Fig. 2 shows the schematic view of the high-speed camera in the cross-section of the central-cell. The high-speed camera observes the plasma behavior on z -axis including the central-limiter through a horizontal port and is sufficiently capable of measuring the light emission with a band of wavelength in visible ranges. The light emission mainly arises from the interaction between plasma and the central-limiter.

A microwave interferometer and a diamagnetic loop are installed near the midplane of the central cell to measure the electron line-density (NL_{cc}) and the diamagnetism (DM_{cc}) in the central-cell.

2.3 Experiment of antenna optimization in the central-ECRH system

The C-ECRH pulse is injected into the plasma for the bulk electron heating in the central-cell. As shown in Fig. 3, the microwave of C-ECRH (28 GHz - 400 kW) is launched to mirror throat region between the central-cell and the east anchor-cell. The microwave power is absorbed near a fundamental harmonic region around $z = -240$ cm. In 2008, the antenna of C-ECRH has been upgraded as a vertical steering function from a fixed type in order to opti-

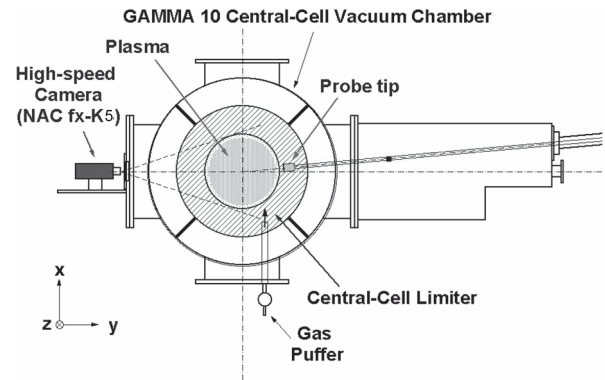


Fig. 2 Schematic view of the central-cell cross-section and the location of the high-speed camera.

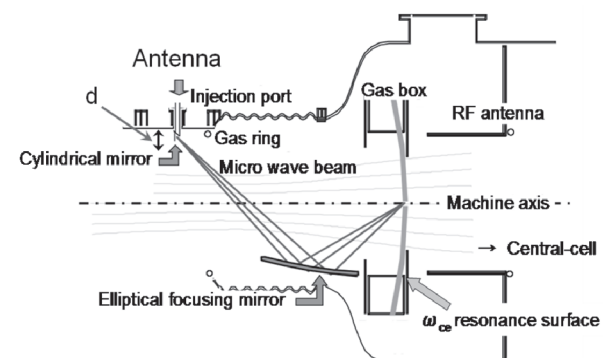


Fig. 3 Schematic view of central-ECRH Injection.

mize the C-ECRH launching condition experimentally [9]. The standard position of C-ECRH antenna is defined as $d = 0$ mm, which is determined from the calculation of microwave propagation. Upper and lower directions of the antenna correspond to plus and minus, respectively. According to the antenna position, focal point in the plasma moves vertically in the range of ± 10 mm in the same direction. We investigated the dependence of the plasma performance during C-, P-, and B-ECRH on the antenna position. In typical Hot-ion-mode plasmas, C-ECRH is injected in the period of P-/B-ECRHs for confining plasma.

3. Experimental Results

Fig. 4 shows the time behavior of DM_{cc} and NL_{cc} during all ECRHs in the discharge with each position of the antenna of C-ECRH ((a) $d = +10$ and (b) $d = -9$ mm). It is recognized that DM_{cc} gradually increases along with the pulses of P-ECRH and C-ECRH in the both cases. However, DM_{cc} turns to decrease near $t = 185$ ms in the course of applying all ECRHs in the higher antenna position ($d = +10$ mm) as shown in Fig. 4 (a). On the other hand, in the case of lower position ($d = -9$ mm), there are no decrease of DM_{cc} during all ECRHs as shown in Fig. 4 (b).

Fig. 5 (a) shows an example of 2-D image of plasma. It shows that the light emission arises strongly from the

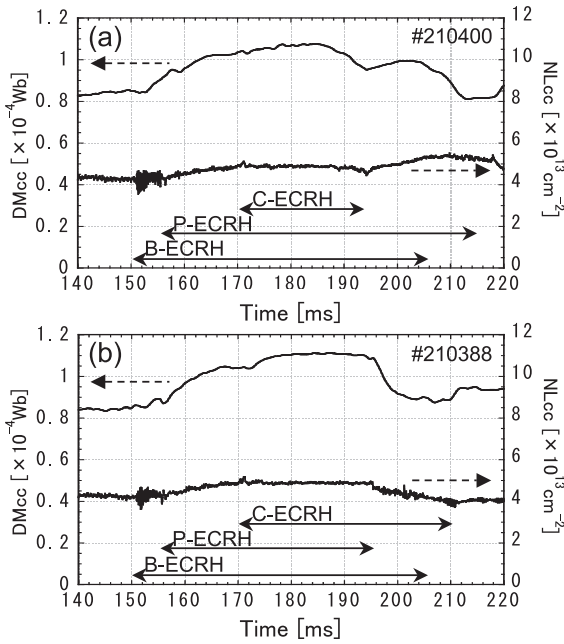


Fig. 4 Time behavior of plasma parameters; Diamagnetism (DMcc), electron line density (NLcc) in the central-cell. Antenna position: (a) $d = +10$ mm, (b) $d = -9$ mm.

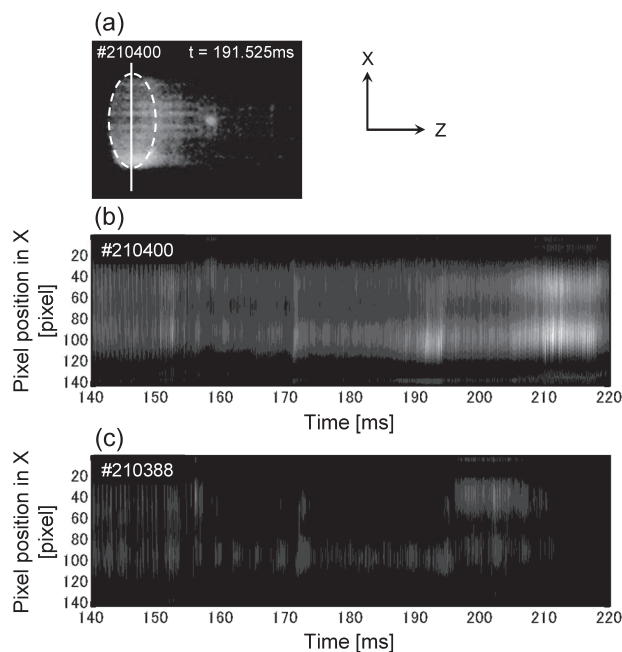


Fig. 5 (a): An example of 2-D image of plasma. Time evolution of the light emission intensity on the vertical pixels (white line in (a)) including the edge of the central-limiter (white dashed circle): (b) $d = +10$ mm, (c) $d = -9$ mm.

bottom of the central-limiter (white dashed circle). The time evolution of the light emission intensity on vertical pixels (white line in the figure) including the edge of the central-limiter is shown in Fig. 5 (b) and (c). In the case of higher antenna position ($d = +10$ mm), as shown in Fig. 5 (b), it is found that light emission during all ECRHs

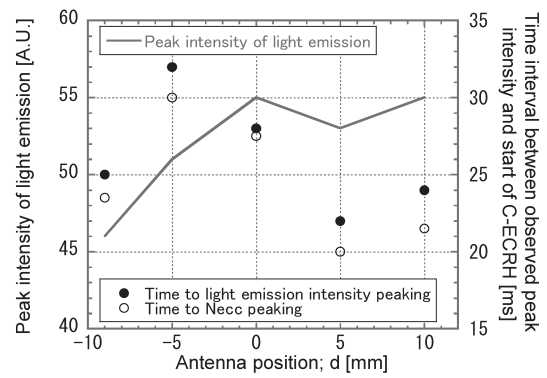


Fig. 6 Dependence of the antenna position on the peak intensity of the light emission and the intervals between the time observed at the peak intensity and the start time of C-ECRH injection.

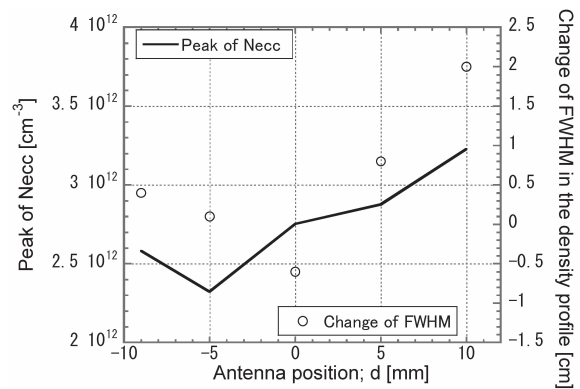


Fig. 7 The peak value of Necc and change of FWHM of radial distribution of Necc.

increases gradually near the bottom of the central-limiter at the same time that DMcc begins to decrease. It suggests that plasma energy is lost by charge-exchange reaction due to the enhancement of hydrogen recycling near the bottom of the central-limiter. On the other hand, in the case of lower position ($d = -9$ mm), the intensity of the light emission is low during all ECRHs and there are no increase of the light emission from the bottom of the limiter as shown in Fig. 5 (b).

The dependence of the peak intensity of the light emission during all ECRHs is plotted on the C-ECRH antenna position in Fig. 6. The intervals between the time observed at the peak intensity and the start time of C-ECRH injection are also plotted. The peak value of the light emission tends to increase according to the height of the antenna position. It is also found that the peaking time of the light emission (filled circle) reaches after the peaking time of the central value in the electron density (open circle) determined from the radial profile measurement of NLcc. The time difference from peaking of Necc to peaking of the light emission has little dependence on the antenna position.

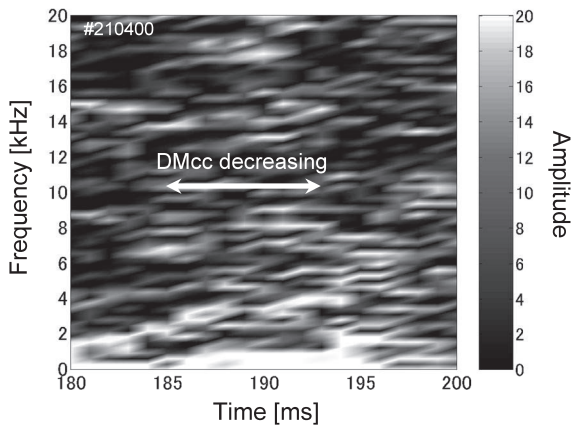


Fig. 8 Frequency of the visible light fluctuation near the bottom of the central-limiter by FFT analysis.

The dependence of the time evolution of the radial profile in the electron density on the antenna position is examined during all ECRHs. As shown in Fig.7, the change in FWHM value of $N_{\text{ecc}}(r)$ and its peak value are plotted as a function of the antenna position. It is revealed that higher position of the antenna tends to contribute to higher electron density plasma production in the central-cell. It is also found that the electron density distribution tends to expand more widely according to the height of the antenna position.

4. Discussion

From the experimental results, DM_{cc} increases together with the start of all ECRHs in every positions of the C-ECRH antenna. However, in higher antenna position, DM_{cc} turns to decrease in the course of applying all ECRHs at the same time that N_{ecc} radial distribution expands widely. Then the light emission arises strongly near the bottom of the central-limiter. This phenomenon of the light emission takes place after the peaking of N_{ecc} . It is also found that the higher antenna position has a tendency to produce the higher N_{ecc} . After N_{ecc} increases to a certain upper limit, its radial distribution is flattened, which suggests the enhancement of radial particle transport in this period. At present, outward particle flux is not measured yet. However, it can be consistently explained from this

mechanism that edge N_{ecc} increases and the light emission arises strongly due to the interaction between edge plasma and the bottom of the central-limiter. It also suggests that this phenomenon causes degradation of the stored energy.

The frequency of the light emission fluctuation near the bottom of central-limiter observed in the case of higher antenna position is investigated by Fourier analysis. As shown in Fig. 8, low-frequency fluctuation (1-6 kHz) is observed to be dominant in the period that DM_{cc} is decreasing. The relationship between these frequencies of fluctuation and above mentioned radial transport mechanism is not clarified yet.

5. Summary

The two-dimensional (2-D) imaging of the plasma behavior in the experiment of antenna optimization in the central-ECRH system was measured at the central-cell by using a high-speed camera in the GAMMA 10 Tandem Mirror. 2-D diagnostics using high-speed cameras are proved to be a useful tool for the optimization of the plasma production and heating. In this study, it is revealed that antenna position of C-ECRH is important for the plasma heating.

Acknowledgement

This study is supported by the bi-directional collaboration researches with Hiroshima University and NIFS (NIFS09KUGM033). The authors would like to acknowledge the members of GAMMA 10 group, University of Tsukuba for their help in the experiment.

- [1] S. J. Zweben *et al.*, Phys. Plasmas **9**, 1981 (2002).
- [2] R. J. Maqueda and G. A. Wurden *et al.*, Rev. Sci. Instrum. **74** (3), 2020 (2003).
- [3] N. Nishino *et al.*, J. Nucl. Mater. **337-339**, 1073 (2005).
- [4] N. Nishino *et al.*, J. Plasma Fusion Res. **1**, 035 (2006).
- [5] Y. Nakashima *et al.*, Trans. Fusion Sci. Technol. **51**, No.2T, 82 (2007).
- [6] Y. Nakashima *et al.*, J. Nucl. Mater. **363-365**, 616 (2007).
- [7] Y. Nakashima *et al.*, Plasma Fusion Res. **2**, S1056 (2007).
- [8] M. Inutake *et al.*, Phys. Rev. Lett. **55**, 939 (1985).
- [9] H. Shidara *et al.*, Trans. Fusion Technol. **55**, 2T, 131-5 (2009).